Equation of state and liquid-vapor equilibria of one- and two-Yukawa hard-sphere chain fluids: Theory and simulation

Yurij V. Kalyuzhnyi
Institute for Condensed Matter Physics, Svientsitskoho 1, 79011 Lviv, Ukraine

Clare McCabe[a] and Eric Whitebay
Department of Chemical Engineering, Colorado School of Mines, Golden, Colorado 80401

Peter T. Cummings
Department of Chemical Engineering, Vanderbilt University, Nashville, Tennessee 37235-1604 and Chemical Sciences Division and Center for Nanophase Materials Sciences, Oak Ridge National Laboratory, Oak Ridge, Tennessee 37831-6110

(Received 14 June 2004; accepted 2 August 2004)

The accuracy of several theories for the thermodynamic properties of the Yukawa hard-sphere chain fluid are studied. In particular, we consider the polymer mean spherical approximation (PMSA), the dimer version of thermodynamic perturbation theory (TPTD), and the statistical associating fluid theory for potentials of variable attractive range (SAFT-VR). Since the original version of SAFT-VR for Yukawa fluids is restricted to the case of one-Yukawa tail, we have extended SAFT-VR to treat chain fluids with two-Yukawa tails. The predictions of these theories are compared with Monte Carlo (MC) simulation data for the pressure and phase behavior of the chain fluid of different length with one- and two-Yukawa tails. We find that overall the PMSA and TPTD give more accurate predictions than SAFT-VR, and that the PMSA is slightly more accurate than TPTD. © *2004 American Institute of Physics.* [DOI: 10.1063/1.1798054]

I. INTRODUCTION

This is the fourth in a series of papers[1–3] on the structure and thermodynamic properties of Yukawa hard-sphere chain fluids. In the previous three papers the pressure-volume-temperature (PVT) and phase behavior, and site-site pair distribution functions were studied using the polymer mean spherical approximation[4–7] (PMSA) and molecular simulation. The PMSA corresponds to the MSA version of the product-reactant Ornstein-Zernike approach[7–11] (PROZA), which in turn originates from the multidensity integral-equation theory for associating fluids developed by Wertheim.[12,13] The PROZA is a theory that yields monomer-monomer pair correlation functions, from which the thermodynamics of a model fluid of polymer molecules can be obtained. In the first two papers in this series[1,2] the analytical solution of the PMSA for one-component multi-Yukawa hard-sphere chain molecules [molecules with additional site-site interaction represented by the multiple sum of the Yukawa tails outside the hard core, see Eq. (1)] was given and closed form analytical expressions for the thermodynamical properties of the model were derived. In the third paper[3] we extended our solution of the PMSA to the general case of a multicomponent multi-Yukawa hard-sphere chain fluid. To validate the accuracy of the theory, Monte Carlo (MC) computer simulations were carried out and the results compared systematically with the theoretical results for the structure and PVT properties of the one-Yukawa version of the model. In general it was found that the theory performs very well, thus providing an analytical route to the equilibrium properties of a well-defined model for chain fluids.

In the present study we focus on the investigation of the PVT behavior and liquid-vapor phase equilibria of one- and two-Yukawa chain fluids. We compare the results of MC computer simulations with several different theoretical approaches, namely, the PMSA, the dimer version of thermodynamic perturbation theory (TPTD), and the statistical associating fluid theory[14,15] for potentials of variable attractive range (SAFT-VR).[16,17] Within the SAFT-VR approach proposed by Gil-Villegas *et al.*,[16,17] the thermodynamic properties of the one-Yukawa chain fluid can be described. Here we extend the SAFT-VR method to treat multi-Yukawa chain fluids and propose corresponding extensions of the TPTD approach.[18,19] Predictions from these theoretical methods are then systematically compared against computer simulation data and the predictions of the PMSA. The paper is organized as follows: In Sec. II we present the model and theories studied, followed by details of the simulations performed in Sec. III. The results of comparisons between the theoretical predictions and simulation data are presented in Sec. IV and concluding remarks made in Sec. V.

II. THE MODEL AND THEORY

We consider a one-component fluid of freely-jointed tangent hard-sphere Yukawa chain (HSYC) molecules with a number density $\rho = N/V$. Each molecule is represented by m tangentially bonded hard-sphere Yukawa monomers (sites) of equal hard-core diameter σ. Nonbonded monomers, regardless of whether they belong to the same molecule or to the

[a]Present address: Department of Chemical Engineering, Vanderbilt University, Nashville, TN 37235-1604. Electronic mail: c.mccabe@vanderbilt.edu

TABLE I. Parameters of the one-Yukawa (1Ya,1Yb) and two-Yukawa (2Y) model potentials.

Model	$z_1\sigma$	$z_2\sigma$	$(K^{(1)}/\sigma\beta^*)\,e^{-z_1\sigma}$	$(K^{(2)}/\sigma\beta^*)\,e^{-z_2\sigma}$
1Ya	1.800	⋯	−1.000	⋯
1Yb	3.000	⋯	−1.000	⋯
2Y	2.673	4.408	−4.755	3.955

different molecules, interact directly via the hard-sphere interaction $\Phi^{(hs)}(r)$ and Yukawa potential $\Phi^{(Y)}(r)$,

$$\Phi(r)=\Phi^{(hs)}(r)+\Phi^{(Y)}(r), \tag{1}$$

where

$$\beta\Phi^{(Y)}(r)=-\frac{1}{r}\sum_{m}^{N_Y} K_m e^{-z_m r}, \tag{2}$$

with $\beta=1/kT$ and r the center-to-center separation between two monomer beads.

A. PMSA

In this study we use the PROZA with the PMSA closure. The present version of PROZA consists of an Ornstein-Zernike-like integral equation, which in Fourier space has the form

$$\hat{\mathbf{h}}_{ij}(k)=\hat{\mathbf{c}}_{ij}(k)+\rho\sum_{l}\hat{\mathbf{c}}_{il}(k)\boldsymbol{\alpha}\cdot\mathbf{h}_{lj}(k), \tag{3}$$

and the PMSA boundary conditions, which are given by

$$\begin{cases}\mathbf{c}_{ij}(r)=\mathbf{E}\sum_{m}\dfrac{K_m}{r}e^{-z_m r}, & r>\sigma\\ \mathbf{h}_{ij}(r)=-\mathbf{E}+\dfrac{\mathbf{t}_{ij}}{2\pi\sigma}\delta(r-\sigma), & r<\sigma.\end{cases} \tag{4}$$

Here the indices i and j denote the species (position) of the monomers in the chain, $\hat{h}_{ij}(k)$ and $\hat{c}_{ij}(k)$ are matrices with

TABLE II. Isothermal-isobaric Monte Carlo simulation results for the hard-core two-Yukawa dimer fluid. The fixed variables during the simulation are the number of particles $N=256$, the reduced pressure $p^*=p\sigma^3/\varepsilon$, and the reduced temperature $T^*=kT/\varepsilon$, where ε is the depth of the two-Yukawa potential and σ is the hard-sphere diameter. The packing fraction is given by η and intermolecular configurational energy ΔE per chain molecule by $\Delta E/NkT$; the uncertainties correspond to one standard deviation. $g(\sigma^+)$ denotes the contact value of the site-site radial distribution function.

T^*	p^*	η	$\Delta E/NkT$	$g(\sigma^+)$
1.8	0.96	0.382±0.008	−7.45±0.17	2.17
1.8	2.68	0.421±0.006	−8.32±0.13	2.69
3.0	0.22	0.120±0.012	−1.32±0.14	1.11
3.0	0.70	0.237±0.012	−2.62±0.15	1.32
3.0	2.26	0.321±0.008	−3.67±0.11	1.76
3.0	4.89	0.376±0.007	−4.39±0.10	2.21
3.0	8.90	0.423±0.006	−5.00±0.08	2.79
5.0	0.66	0.116±0.012	−0.72±0.06	0.94
5.0	1.76	0.208±0.012	−1.33±0.07	1.17
5.0	5.28	0.305±0.008	−2.07±0.06	1.65
5.0	10.71	0.370±0.007	−2.58±0.05	2.21
5.0	17.90	0.415±0.006	−2.94±0.04	⋯

elements that are Fourier transforms of the elements of the real-space matrices $\mathbf{h}_{ij}(r)$ and $\mathbf{c}_{ij}(r)$, defined by

$$\mathbf{f}_{ij}(r)=\begin{pmatrix} f_{i_0j_0}(r) & f_{i_0j_A}(r) & f_{i_0j_B}(r)\\ f_{i_Aj_0}(r) & f_{i_Aj_A}(r) & f_{i_Aj_B}(r)\\ f_{i_Bj_0}(r) & f_{i_Bj_A}(r) & f_{i_Bj_B}(r)\end{pmatrix},$$

$$\mathbf{f}_{ij}(r)=\mathbf{h}_{ij}(r),\ \ \mathbf{c}_{ij}(r).$$

In this equation, the quantities $h_{i_\alpha j_\beta}(r)$ and $c_{i_\alpha j_\beta}(r)$ appearing in $\mathbf{h}_{ij}$ and $\mathbf{c}_{ij}(r)$, respectively, represent partial total and direct correlation functions. The lower indices α and β each take the values 0, A, and B, and denote the bonding states of the corresponding particles, i.e., the case of $\alpha=0$ corre-

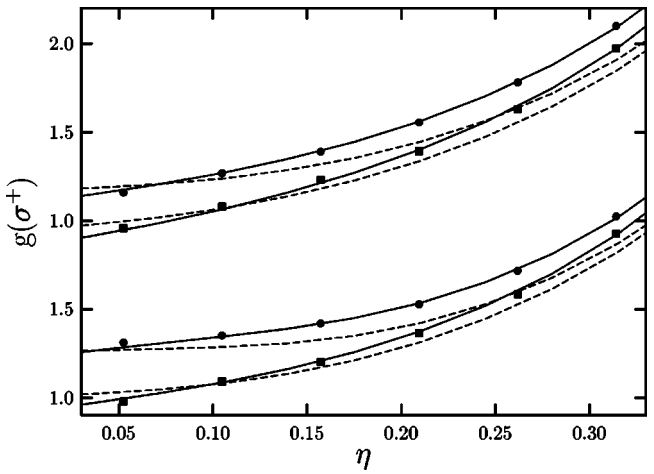

FIG. 1. Contact values of site-site pair distribution function of Yukawa dimer fluid vs η for $z\sigma=1.8$ (lower portion of the figure) and $z\sigma=3$ (upper portion of the figure) at $T^*=2$ (circles) and $T^*=3$ (squares). Symbols are from the MC simulation (Ref. 43), solid curves are from approximation (14), and dashed curves are from the PMSA.

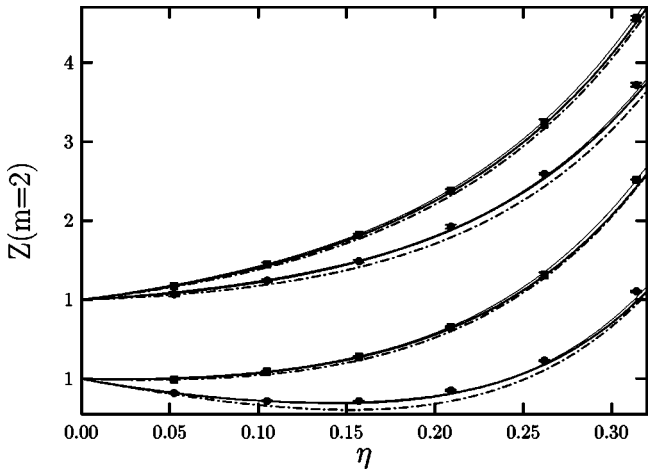

FIG. 2. Compressibility factor $Z=\beta P/\rho$ of one-Yukawa dimer fluid with $z\sigma=1.8$ (1Ya model, lower portion of the figure) and $z\sigma=3$ (1Yb model, upper portion of the figure) at $T^*=2$ (circles) and $T^*=3$ (squares). Symbols are from the MC simulation (Ref. 43), solid and dashed-dotted curves represent PMSA and SAFT-VR results, respectively.

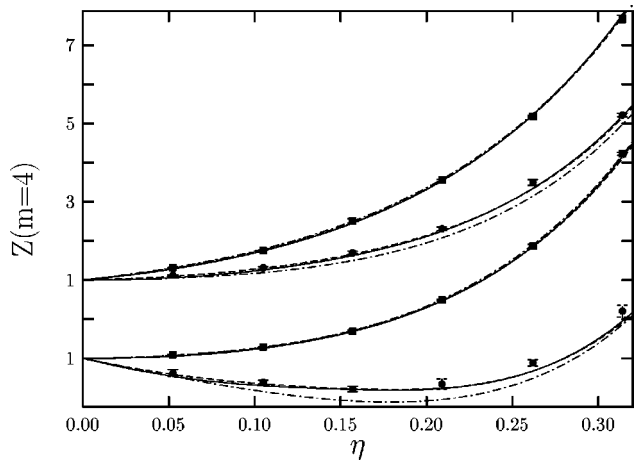

FIG. 3. Compressibility factor $Z=\beta P/\rho$ of one-Yukawa 4-mer fluid with $z\sigma=1.8$ (1Ya model, lower portion of the figure) and $z\sigma=3$ (1Yb model, upper portion of the figure) at $T^*=2$ (circles) and $T^*=4$ (squares). Symbols are from the MC simulation (Ref. 43), solid and dashed-dotted curves represent PMSA and SAFT-VR results, respectively, and dashed curves represent TPTD results.

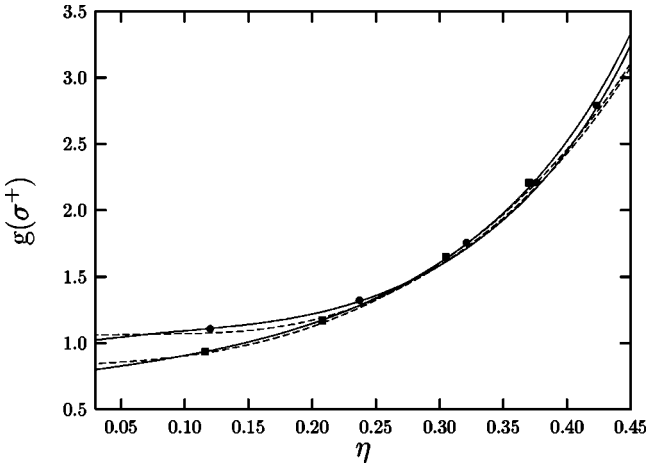

FIG. 5. Contact values of site-site pair distribution function of the 2Y model of Yukawa dimer fluid vs η at $T^*=3$ (circles) and $T^*=5$ (squares). Symbols are from the MC simulation, solid curves are from approximation (14), and dashed curves are from the PMSA.

sponds to an unbonded particle, while $\alpha=A$ or $\alpha=B$ to A-bonded or B-bonded particle, respectively. The quantities $\mathbf{t}_{ij}$, $\boldsymbol{\alpha}$, and $\mathbf{E}$ are the following matrices:

$$t_{i_\alpha j_\beta}=\frac{1}{2\rho\sigma}[\delta_{\alpha A}\delta_{\beta B}\delta_{i,j+1}+\delta_{\alpha B}\delta_{\beta A}\delta_{i,j-1}], \tag{5}$$

$$\alpha_{\alpha\beta}=1-\delta_{\alpha\beta}+\delta_{\alpha 0}\delta_{\beta 0}, \tag{6}$$

$$E_{\alpha\beta}=\delta_{\alpha 0}\delta_{\beta 0}. \tag{7}$$

Here the matrix $\mathbf{t}_{ij}$ specifies the sequence of monomer species for the monomers which form a chain molecule.

The site-site pair distribution function $h_{ij}(r)$ is related to the partial distribution functions $g_{i_\alpha j_\beta}(r)=h_{i_\alpha j_\beta}(r)+\delta_{\alpha 0}\delta_{\beta 0}$ by the relation

$$g_{ij}(r)=\sum_{\alpha,\beta=0} g_{i_\alpha j_\beta}(r). \tag{8}$$

The set of the Ornstein-Zernike equations (3) together with the PMSA closure conditions (4) represent a closed set of equations solved in our previous publications.[1–3] This solution was then used to derive closed form analytical expressions for the thermodynamic properties of the model at hand. To avoid unnecessary repetition, we do not present the solution and thermodynamic expressions here, for details the reader is referred to the original publications.[1–3]

B. SAFT-VR

Following Wertheim's TPT for associating fluids[12,13,20] in the SAFT-VR (Ref. 16) approach for chain fluids it is assumed that the Helmholtz free energy A can be written as a linear sum of the ideal, monomer, and chain contributions,

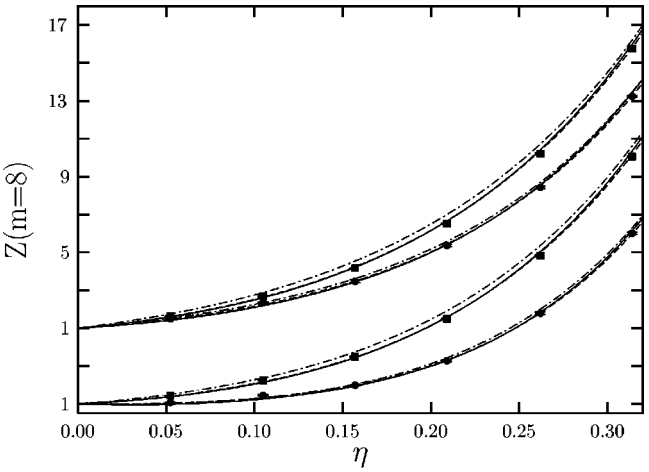

FIG. 4. Compressibility factor $Z=\beta P/\rho$ of one-Yukawa 8-mer fluid with $z\sigma=1.8$ (1Ya model, lower portion of the figure) and $z\sigma=3$ (1Yb model, upper portion of the figure) at $T^*=4$ (circles) and $T^*=8$ (squares). Symbols are from the MC simulation (Ref. 43), solid and dashed-dotted curves represent PMSA and SAFT-VR results, respectively, and dashed curves represent TPTD results.

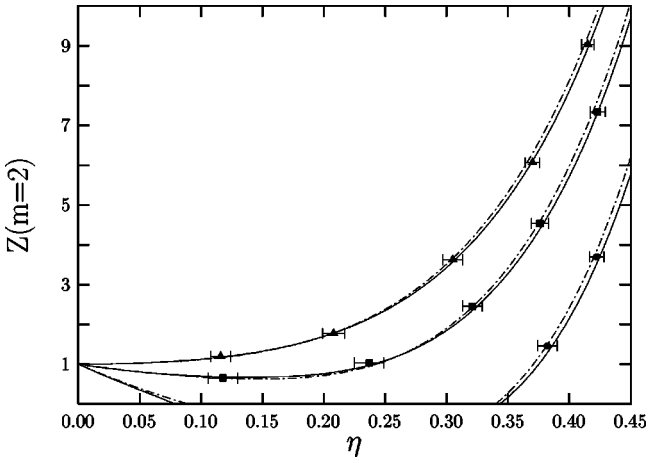

FIG. 6. Compressibility factor $Z=\beta P/\rho$ of two-Yukawa dimer fluid (2Y model) at $T^*=1.8$ (circles), $T^*=3$ (squares), and $T^*=5$ (triangles). Symbols are from the MC simulation, solid and dashed-dotted curves represent PMSA and SAFT-VR results, respectively.

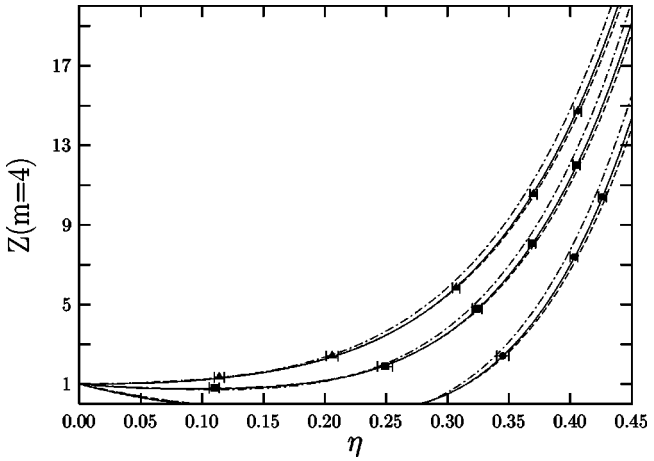

FIG. 7. Compressibility factor $Z=\beta P/\rho$ of two-Yukawa 4-mer fluid (2Y model) at $T^*=2.6$ (circles), $T^*=4$ (squares), and $T^*=6$ (triangles). Symbols are from the MC simulation, solid and dashed-dotted curves represent PMSA and SAFT-VR results, respectively, and dashed curves represent TPTD results.

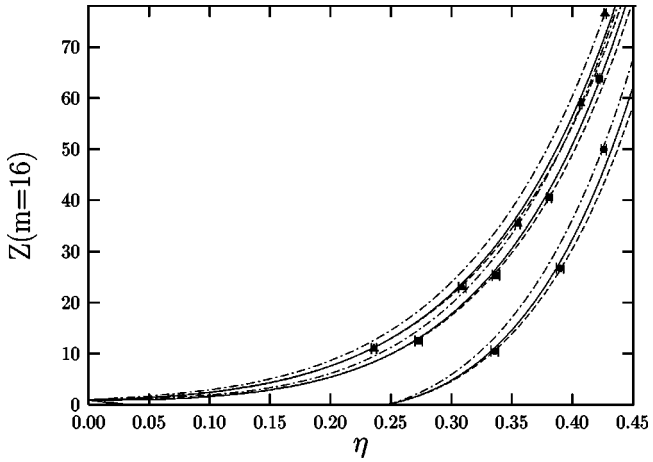

FIG. 9. Compressibility factor $Z=\beta P/\rho$ of two-Yukawa 16-mer fluid (2Y model) at $T^*=3.2$ (circles), $T^*=5.2$ (squares), and $T^*=8.2$ (triangles). Symbols are from the MC simulation, solid and dashed-dotted curves represent PMSA and SAFT-VR results, respectively, and dashed curves represent TPTD results.

$$\frac{\beta A}{N}=\frac{\beta A^{(Ideal)}}{N}+\frac{\beta A^{(Mono.)}}{N}+\frac{\beta A^{(Chain)}}{N}, \tag{9}$$

where N is the number of molecules in the system, and

$$\frac{\beta A^{(Ideal)}}{N}=\ln(\rho\Lambda^3)-1, \tag{10}$$

where Λ is the thermal de Broglie wavelength. The free energy due to monomer segments is given by

$$\frac{\beta A^{(Mono.)}}{N}=m a^{(Mono.)}, \tag{11}$$

where $a^{(Mono.)}$ is the excess Helmholtz free energy per monomer of a system of (nonbonded) Yukawa monomers and is treated via a second-order high-temperature perturbation expansion, providing a more rigorous description of the thermodynamics than found in simpler versions of the SAFT approach.[16] The monomer segments are then bonded to form chains giving

$$\frac{\beta A^{(Chain)}}{N}=-(m-1)\ln y^{(Mono.)}(\sigma), \tag{12}$$

where $y^{(Mono.)}(\sigma)$ is the contact value of the monomer-monomer background (or cavity) distribution function for a system of nonbonded Yukawa monomers. In general, $y^{(Mono.)}(r)=e^{\beta\Phi^Y(r)}g^{(Mono.)}(r)$, where $g^{(Mono.)}(r)$ is the monomer-monomer radial distribution function, so that $y^{(Mono.)}(\sigma)=e^{\beta\Phi^{(Y)}(\sigma)}g^{(Mono.)}(\sigma)$. We note that in this work we do not consider the association term which is used in the modeling of real fluids to mimic molecular interactions such as hydrogen bonding. Thus SAFT-VR uses as input information on the structure and thermodynamic properties of the reference fluid. The reference fluid in the SAFT-VR approach is described by a potential model of variable attrac-

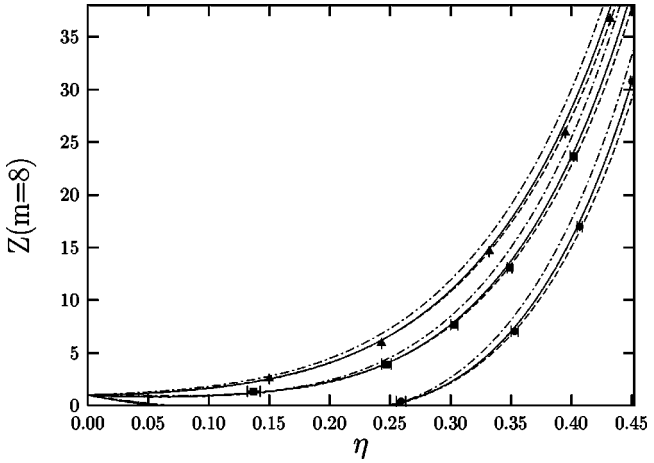

FIG. 8. Compressibility factor $Z=\beta P/\rho$ of two-Yukawa 8-mer fluid (2Y model) at $T^*=3.2$ (circles), $T^*=5.2$ (squares), and $T^*=8.2$ (triangles). Symbols are from the MC simulation, solid and dashed-dotted curves represent PMSA and SAFT-VR results, respectively, and dashed curves represent TPTD results.

TABLE III. Isothermal-isobaric Monte Carlo simulation results for the hard-core two-Yukawa 4-mer fluid. The fixed variables during the simulation are as for Table II.

T^*	p^*	η	$\Delta E/NkT$
2.6	1.03	0.345±0.005	−8.81±0.14
2.6	3.70	0.403±0.003	−10.56±0.08
2.6	5.50	0.426±0.003	−11.25±0.07
4.0	0.17	0.110±0.004	−1.87±0.7
4.0	0.90	0.249±0.006	−3.93±0.11
4.0	2.96	0.324±0.004	−5.31±0.08
4.0	5.69	0.369±0.003	−6.18±0.07
4.0	9.29	0.405±0.003	−6.89±0.06
6.0	0.44	0.114±0.004	−1.17±0.05
6.0	1.42	0.206±0.005	−2.10±0.06
6.0	5.13	0.307±0.003	−3.31±0.04
6.0	11.17	0.370±0.003	−4.13±0.04
6.0	17.10	0.406±0.003	−4.61±0.04

TABLE IV. Isothermal-isobaric Monte Carlo simulation results for the hard-core two-Yukawa 8-mer fluid. The fixed variables during the simulation are as for Table II.

T^*	p^*	η	$\Delta E/NkT$
3.2	0.08	0.259±0.004	−10.21±0.18
3.2	1.90	0.353±0.003	−14.35±0.88
3.2	5.28	0.407±0.002	−17.05±1.02
3.2	10.58	0.450±0.001	−19.12±1.12
5.2	0.23	0.137±0.005	−3.37±0.11
5.2	1.20	0.247±0.004	−5.81±0.38
5.2	2.89	0.303±0.003	−7.34±0.47
5.2	5.66	0.349±0.002	−8.69±0.54
5.2	11.80	0.402±0.003	−10.32±0.62
8.2	0.74	0.150±0.003	−2.17±0.04
8.2	2.80	0.243±0.003	−3.56±0.24
8.2	9.50	0.332±0.002	−5.19±0.32
8.2	20.00	0.395±0.002	−6.41±0.39
8.2	31.00	0.432±0.002	−7.11±0.42
2.50	0.0001	0.328±0.004	−16.83±0.35
2.75	0.0005	0.299±0.005	−13.70±0.23
3.00	0.0018	0.269±0.005	−11.33±0.19
2.6	0.0002	0.315±0.005	−15.55±0.28
2.9	0.0011	0.280±0.005	−12.27±0.24

tive range. In particular, the the square well potential has been used extensively to describe both model[17,21] as well as real chain fluids.[22–32]

In the original application of SAFT-VR to Yukawa fluids[16] the monomer Helmholtz free energy and pair distribution function were determined from second- and first-order Barker-Henderson perturbation theory, respectively.[33,34] The reference system was a hard-sphere fluid, whose structural properties were computed using a highly accurate version of the hard-sphere fluid structure, i.e., the Malijevksy-Labik integral-equation theory.[35] More recently Davies *et al.* proposed combining the SAFT-VR approach with the MSA high-temperature expansion[36] (HTE), providing a completely analytical equation of state. Comparison of the original SAFT-VR approach, MSA-HTE, and a combination of both the SAFT-VR and MSA approaches with simulation data determined that the most accurate equation of state was obtained when a combination of the MSA-HTE and SAFT-VR was used. However, since the MSA-HTE is restricted to the one-component one-Yukawa case, in the present study we use the results of the MSA directly. This allows the description of both one- and two-Yukawa chain fluids within the SAFT-VR framework. The MSA Helmholtz free energy, equation of state, chemical potential, and pair distribution function can be calculated using Blum and Høye's[37] solution of the MSA and Høye and Stell's[38] route to the MSA thermodynamics. Corresponding expressions for the multicomponent multi-Yukawa hard-sphere fluid in their ready-to-use form have been developed by Arrieta *et al.*[39] In the Appendix

TABLE V. Isothermal-isobaric Monte Carlo simulation results for the hard-core two-Yukawa 16-mer fluid. The fixed variables during the simulation are as for Table II.

T^*	p^*	η	$\Delta E/NkT$
3.5	1.47	0.336±0.003	−24.47±0.28
3.5	4.35	0.390±0.002	−29.29±0.15
3.5	8.89	0.426±0.001	−32.49±0.07
7.0	2.86	0.273±0.003	−9.48±0.12
7.0	7.13	0.337±0.003	−12.21±0.13
7.0	12.90	0.381±0.002	−14.19±0.11
7.0	22.50	0.422±0.001	−16.04±0.05
10.0	3.09	0.236±0.002	−5.57±0.06
10.0	8.47	0.309±0.003	−7.67±0.10
10.0	15.00	0.355±0.002	−9.11±0.08
10.0	28.60	0.407±0.001	−10.77±0.04
10.0	39.00	0.427±0.001	−11.41±0.02

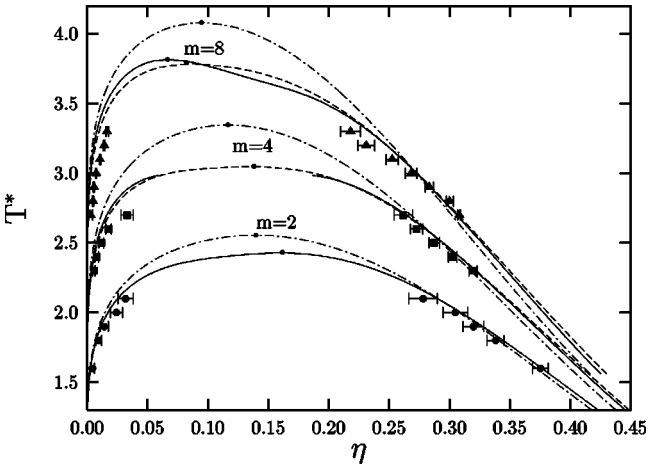

FIG. 10. The liquid-vapor coexistence curves for two-Yukawa chain fluid (2Y model) of the chain length $m=2,4,8$ (from the bottom to the top). Symbols are from the MC simulation, solid curves represent PMSA predictions, dashed-dotted curves represent SAFT-VR predictions, and dashed curves represent TPTD predictions. Small filled circle on the top of each coexistence curve shows the location of the corresponding critical point.

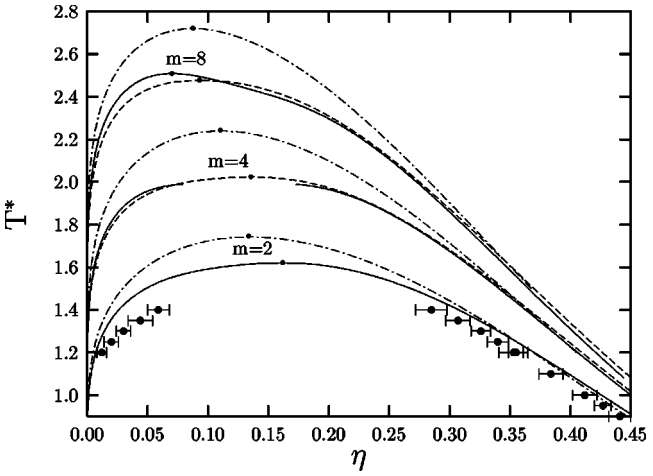

FIG. 11. The liquid-vapor coexistence curves for one-Yukawa chain fluid (1Ya model) of the chain length $m=2,4,8$ (from the bottom to the top). Symbols are from the MC simulation for $m=2$, solid curves represent PMSA predictions, dashed-dotted curves represent SAFT-VR predictions, and dashed curves represent TPTD predictions. Small filled circle on the top of each coexistence curve shows the location of the corresponding critical point.

TABLE VI. Vapor-liquid coexistence data obtained from *NVT* Gibbs ensemble Monte Carlo simulations for the 2Y model with $m=2,4,8$. The vapor and liquid packing fractions are denoted as v and l, respectively. See Table II for the definition of the remaining symbols.

T^*	η_v	η_l	$\Delta E_v/NkT$	$\Delta E_l/NkT$	N_v	N_l
			$m=2$			
1.6	0.004±0.002	0.375±0.006	−0.135±0.144	−8.238±0.161	8	248
1.8	0.009±0.002	0.338±0.007	−0.256±0.140	−6.518±0.163	18	238
1.9	0.014±0.003	0.320±0.009	−0.348±0.144	−5.804±0.171	26	230
2.0	0.024±0.005	0.305±0.010	−0.560±0.166	−5.230±0.189	45	211
2.1	0.032±0.006	0.278±0.012	−0.673±0.173	−4.514±0.200	49	207
			$m=4$			
2.3	0.006±0.001	0.319±0.003	−0.816±0.156	−9.149±0.105	19	493
2.4	0.008±0.002	0.302±0.004	−0.855±0.150	−8.257±0.107	28	484
2.5	0.012±0.002	0.287±0.004	−0.944±0.148	−7.492±0.119	37	474
2.6	0.018±0.002	0.273±0.005	−1.153±0.173	−6.820±0.127	56	456
2.7	0.033±0.005	0.262±0.008	−1.594±0.227	−6.285±0.178	73	439
			$m=8$			
2.7	0.003±0.001	0.308±0.001	−2.275±0.607	−15.584±0.072	4	508
2.8	0.005±0.001	0.300±0.003	−2.501±0.207	−14.593±0.158	50	462
2.9	0.006±0.001	0.283±0.004	−2.432±0.170	−13.243±0.175	66	446
3.0	0.008±0.001	0.269±0.001	−2.443±0.128	−12.098±0.209	135	377
3.1	0.011±0.001	0.254±0.005	−2.523±0.136	−11.022±0.214	122	390
3.2	0.014±0.001	0.231±0.007	−2.584±0.130	−9.844±0.253	157	355
3.3	0.016±0.001	0.216±0.001	−2.576±0.133	−8.527±0.244	204	308

we present the expressions used in this work for the one-component case.

C. TPTD

In the context of TPTD, the expression for the Helmholtz free energy (9) can be recast in the following form:[18,19,40]

$$\frac{\beta A}{N}=\frac{\beta A^{(id)}}{N}+\frac{\beta A^{(dim)}}{N}+\left(1-\frac{1}{2}m\right)\ln g_{dim}(\sigma), \tag{13}$$

where $A^{(dim)}$ is the excess Helmholtz free energy for a fluid of Yukawa dimers with hard-sphere diameter σ and molecular density $\rho_{dim}=m\rho/2$, and $g_{dim}(\sigma)$ is the site-site pair distribution function of Yukawa dimers at contact.

In this study, thermodynamic and structural properties of the Yukawa dimer fluid are calculated using the PMSA approach discussed above. To improve the accuracy of the PMSA predictions for $g_{dim}(\sigma)$ we propose an extension of the approximation suggested by Høye and Stell[38] in the framework of the regular MSA approach. Following Høye and Stell,[38] we have

$$\mathbf{g}_{ij}(r)=\mathbf{g}_{ij}^{(0)}(r)+\tfrac{1}{2}\mathrm{Tr}[\mathbf{g}_{ij}(r)\boldsymbol{\alpha}\mathbf{g}_{ji}(r)\boldsymbol{\alpha}-\mathbf{g}_{ij}^{(0)}(r)\boldsymbol{\alpha}\mathbf{g}_{ji}^{(0)}(r)\boldsymbol{\alpha}], \tag{14}$$

where $\mathbf{g}_{ij}(r)$ is the matrix with the elements $g_{i_\alpha j_\beta}(r)$ and $\mathbf{g}_{ij}^{(0)}(r)$ represents the partial pair distribution functions of the chain molecular fluid with Yukawa potential turned off, i.e., $K_n=0$. As for the case of the regular MSA, this choice for the pair distribution functions leads to an expression for the virial pressure that coincides with the pressure obtained via the energy route.[7,38,41]

III. COMPUTER SIMULATION

We have calculated the PVT behavior for the dimer, tetramer, 8-mer, and 16-mer one- and two-Yukawa chain fluids using isothermal-isobaric (NpT) Monte Carlo simulation. The NpT simulations were performed at state conditions that ensured a wide range of temperatures and pressures were examined. Additionally we have determined the fluid phase

TABLE VII. Vapor-liquid coexistence data obtained from *NVT* Gibbs ensemble Monte Carlo simulations for the 1Ya model with $m=2$. The vapor and liquid packing fractions are denoted as v and l, respectively. See Table II for the definition of the remaining symbols.

T^*	η_v	η_l	$\Delta E_v/NkT$	$\Delta E_l/NkT$	N_v	N_l
			$m=2$			
1.20	0.012±0.004	0.355±0.006	−0.278±0.171	−6.688±0.136	13	243
1.25	0.020±0.006	0.340±0.009	−0.444±0.203	−6.106±0.189	21	235
1.30	0.030±0.006	0.326±0.008	−0.614±0.187	−5.591±0.151	26	230
1.35	0.044±0.010	0.307±0.010	−0.867±0.237	−5.016±0.191	53	203
1.40	0.059±0.009	0.285±0.013	−1.070±0.203	−4.442±0.223	52	204

TABLE VIII. Isothermal-isobaric Monte Carlo simulation results for the 1Ya model with $m=2$. The fixed variables during the simulation are as for Table II.

T^*	p^*	η	$\Delta E/NkT$
0.80	0.0001	0.472 ± 0.007	-14.28 ± 0.28
0.85	0.0001	0.455 ± 0.008	-12.85 ± 0.27
0.90	0.0003	0.441 ± 0.009	-11.65 ± 0.29
0.95	0.0007	0.427 ± 0.007	-10.58 ± 0.21
1.00	0.0011	0.412 ± 0.010	-9.64 ± 0.29
1.10	0.0032	0.384 ± 0.010	-8.02 ± 0.26
1.20	0.0076	0.353 ± 0.012	-6.65 ± 0.26

diagram using Gibbs ensemble MC simulation (GEMC) for the one-Yukawa dimer and two-Yukawa dimer, tetramer, and 8-mer fluids.

For the NpT simulations the initial configurations were generated at low pressure by arranging the molecules on a face-centered-cubic lattice; simulations at higher pressure, and hence density, were then started from this equilibrated initial configuration and allowed to reequilibrate to the corresponding density. The simulations were performed with $N=256$ molecules for all fluids except the 16-mer for which $N=128$ was used. For the GEMC simulations the initial configurations were taken from equilibrated NpT runs at either densities approximately mid way between those for the liquid and vapor phase at each state condition or close to the corresponding theoretical solutions. Simulations of the dimer fluids were performed with $N=256$ molecules, while simulations of the 4-mer and 8-mer fluids were performed with $N=512$ molecules. The usual periodic boundary conditions and minimum image convention are applied, with the potential being truncated beyond 3σ in all cases.

In both the NpT and GEMC simulations one simulation cycle consists of N attempted MC moves, one attempted volume change, and a specific number of attempted regrowths (NpT) or insertions (GEMC) of randomly selected molecules using continuum configurational bias sampling.[42] The N MC moves were randomly chosen from displacement, reorientation, and reptation steps in each cycle. In all the simulations the maximum displacement and volume changes were adjusted to give an acceptance ratio of between 30% and 40%, and the number of regrowths were controlled so that between 1% and 3% of the molecules are regrown or inserted in each cycle. The thermodynamic properties of the system were obtained as ensemble averages and the errors estimated by determining the standard deviation. An initial simulation of 50 000–200 000 cycles was performed to equilibrate the system, depending upon pressure and chain length, before averaging for between 200 000 and 500 000 cycles.

IV. RESULTS AND DISCUSSION

In this section we compare the theoretical predictions against computer simulation data for the liquid-gas phase equilibria and PVT behavior of one- and two-Yukawa hard-sphere chain fluids. The theoretical methods are represented by the PMSA, SAFT-VR, and TPTD. We do not show results from first-order TPT (Ref. 43) since its predictions are slightly less accurate than those of SAFT-VR.

Parameters defining the one-Yukawa (1Ya,1Yb) and two-Yukawa (2Y) models studied are collected in Table I. Any thermodynamic state of the HSYC model considered here is defined by a set of two parameters, i.e., temperature T and number density ρ. However it is more convenient to use two dimensionless quantities $T^*=1/\beta^*=kT/\epsilon$ and packing fraction $\eta=\pi\rho m\sigma^3/6$, where ϵ is the depth of the Yukawa potential well and σ the hard-sphere diameter.

To validate the accuracy of the approximation for g_{ij} given by Eq. (14), in Figs. 1 and 5 we show the comparison of the contact values of the dimer site-site pair distribution function $g_{dim}(\sigma)$ predicted from MC computer simulations, PMSA, and the approximation given by Eq. (14) at different temperature and packing fraction. The corresponding simulation data for the 1Ya model is due to Wang and Chiew[43] and for the 2Y model is detailed in Table II. From Fig. 1 we note that the PMSA tends to underpredict the contact values at intermediate and high η and overpredicts at low η. In the two-Yukawa case (Fig. 5) the tendency is similar, although the agreement between the PMSA and MC simulation data is better. Predictions using the approximation for g_{ij} [Eq. (14)] substantially improves the PMSA results and agree very well with computer simulation data. Figures 2 and 6 show the compressibility factor for the dimer version of the 1Ya, 1Yb (Ref. 43) (Fig. 2) and 2Y (Fig. 6) models obtained from the PMSA, SAFT-VR, and MC simulation methods. The simulation data for the 2Y model is given in Table II. For the one-Yukawa dimers the PMSA generally agrees very well with the simulation data (Fig. 2); a slight underprediction is observed for higher values of η. The SAFT-VR results are seen to be less accurate, especially at the lower temperatures. A similar tendency holds for the one-Yukawa 4-mer and 8-mer chain fluids (Figs. 3 and 4), i.e., the predictions of the PMSA are very good, except for the lowest temperature and highest packing fractions (Fig. 3) while the SAFT-VR predictions are less accurate. Similar accuracy is observed for the PMSA results for the two-Yukawa chain fluids (Figs. 6–9 and Tables III–V). The corresponding SAFT-VR results are accurate for the two-Yukawa dimers (Fig. 6); however, deviations are observed for the 4-mers, 8-mers, and 16-mers (Figs. 7–9). For the longer chain fluids results from the TPTD approach are also included (Figs. 3, 4, and 7–9). In all the cases studied the accuracy of TPTD predictions are seen to be similar to that of the PMSA predictions.

Finally Figs. 10 and 11 show vapor-liquid phase diagrams for chains of different length for the 2Y and 1Ya models calculated from the PMSA, SAFT-VR, and TPTD theories. The corresponding computer simulation results are presented for the two-Yukawa chain fluid in Fig. 10 and reported in Table VI; preliminary simulation results on the phase envelope of the one-Yukawa dimer fluid are shown in Fig. 11 and reported in Tables VII and VIII. Simulations of the one-Yukawa chain fluid beyond the dimer level are currently underway; due to the enhanced probability of tangential clustering of spheres in the one-Yukawa chain fluid, leading to a higher proportion of rejected configurations in moves involving volume contractions, these simulations are more demanding computationally and require extensive independent checks. As can be seen from the available simu-

lation results, the theory is in very good agreement with the available simulation results for both cases.

For both the one-Yukawa and two-Yukawa models we were not able to get a convergent solution of the PMSA Maxwell construction for 4-mers in the vicinity of the critical point. This feature is similar to that encountered by the hypernetted chain approximation[44–46] and reflects the nonlinear character of the present PMSA approach. As the chain length increases all the theories predict an increase of the critical temperature and decrease of the critical packing fraction. The most substantial decrease of the critical packing fraction with chain length increase is demonstrated by the PMSA phase envelope. The critical temperature as predicted by the SAFT-VR approach is always higher than that of the PMSA and TPTD. Close agreement between PMSA and TPTD predictions for the pressure yields similarly close agreement for the phase envelope predictions of these two theories. The most substantial difference can be seen in the vicinity of the critical point for longer chains ($m=8$), where PMSA gives a lower value for the critical density. For the two-Yukawa dimer phase diagram the PMSA theory and TPTD approach are in good agreement with the simulation data. As the chain length is increased deviations are observed as the theoretical results overpredict the critical point. Similar agreement between theoretical and computer simulation results can be expected for the one-Yukawa phase diagram.

V. CONCLUDING REMARKS

In this work the accuracy of several theories for the thermodynamic properties of hard-sphere Yukawa chain fluids is studied. In particular we consider the PMSA theory,[1–3] the dimer version of TPT (Refs. 18 and 19) (TPTD) and the SAFT-VR approach,[16,17] both extended to treat multi-Yukawa chain fluids. The predictions from these theories have been compared with MC simulation data for the PVT and phase behavior of one- and two-Yukawa chain fluids of different length. We find that the PMSA and TPTD give the most accurate predictions, with PMSA being slightly more accurate.

ACKNOWLEDGMENTS

The authors acknowledge support from the Division of Chemical Sciences, Geosciences, and Biosciences, Office of Basic Energy Sciences, U.S. Department of Energy, under Grant No. FG05-94ER14421 to Vanderbilt University. Additionally C.M.C. and E.W. acknowledge support from the NSF under Grant No. CTS-0319062 and No. CTS-0432499, and for an REU supplement to ANI-0228912.

APPENDIX: MSA THERMODYNAMICS FOR THE ONE-COMPONENT TWO-YUKAWA HARD-SPHERE FLUID

In this appendix we present closed form MSA expressions for the pair distribution function in contact $g(\sigma+)$, incremental Helmholtz free energy ΔA, pressure ΔP, and chemical potential $\Delta\mu$ due to Arrieta *et al.*,[39] specializing them to the one-component multi-Yukawa case.

We have

$$g(\sigma+)=\frac{1}{2\pi\sigma}\left(b-\sum_m C_m\right), \tag{A1}$$

$$\beta\frac{\Delta A}{N}=\beta\frac{U}{N}-\beta\frac{\Delta P}{\rho}+\frac{1}{2}(\chi^{-1}-\chi_0^{-1}), \tag{A2}$$

$$\beta\frac{\Delta P}{\rho}=\frac{\pi}{3}\rho\sigma^3\{[g(\sigma+)]^2-[g_0(\sigma+)]^2\}+J, \tag{A3}$$

$$\beta\Delta\mu=\beta\frac{\Delta A}{N}+\beta\frac{\Delta P}{\rho}, \tag{A4}$$

where expressions for configurational energy U, isothermal compressibility of the Yukawa fluid χ, and isothermal compressibility of the corresponding hard-sphere fluid in Percus-Yewick approximation χ_0 are

$$\beta\frac{U}{N}=-2\pi\rho\left(\sum_m \frac{e_m}{z_m}K_m G_m\right), \tag{A5}$$

$$\chi^{-1}=\left(\frac{A^{(Y)}}{2\pi}\right)^2, \tag{A6}$$

$$\chi_0^{-1}=\left(\frac{A^{(0)}}{2\pi}\right)^2. \tag{A7}$$

Here,

$$g_0(\sigma+)=\frac{b^{(0)}}{2\pi\sigma}, \tag{A8}$$

$$C_n=f_n e_n-D_n, \tag{A9}$$

$$f_n=\frac{2\pi}{z_n^2}\rho G_n D_n, \tag{A10}$$

$$e_n=e^{-z_n\sigma}, \tag{A11}$$

$$b=b^{(0)}(1+M)+A^{(0)}W, \tag{A12}$$

$$b^{(0)}=2\pi\frac{\sigma(1-\xi_3)+\frac{3}{2}\sigma^2\xi_2}{(1-\xi_3)^2}, \tag{A13}$$

$$A^{(Y)}=A^{(0)}(1+M)-\frac{4}{\sigma^2}B^{(0)}W, \tag{A14}$$

$$A^{(0)}=2\pi\frac{(1-\xi_3+3\sigma\xi_2)}{(1-\xi_3)^2}, \tag{A15}$$

$$B^{(0)}=2\pi\frac{-\frac{3}{2}\sigma^2\xi_2}{(1-\xi_3)^2}, \tag{A16}$$

$$\xi_i=\frac{\pi}{6}\rho\sigma^i, \tag{A17}$$

$$M=-\sum_m \frac{1}{z_m^2}\rho\{M_m^{(a)}D_m+[1-M_m^{(a)}e_m]f_m\}, \tag{A18}$$

$$W=\sum_m \frac{1}{z_m^3}\rho\{L_m^{(a)}D_m+[1-L_m^{(a)}e_m]f_m\}, \tag{A19}$$

$$M_n^{(a)}=1+z_n\sigma, \tag{A20}$$

$$L_n^{(a)}=1+z_n\sigma+\tfrac{1}{2}z_n^2\sigma^2, \tag{A21}$$

$$J=\frac{2\pi}{3}\rho\sum_m K_m e_m\left(G'_m-\frac{1}{z_m}G_m\right). \tag{A22}$$

Thus thermodynamical properties of the model at hand is defined by the set of $3N_Y$ parameters D_n, G_n, and G'_n. The set of $2N_Y$ parameters D_n and G_n follow from the solution of the following set of $2N_Y$ algebraic equations:

$$\sum_m A^{(1)}_{mn}G_m D_m D_n+\sum_m A^{(2)}_{mn}D_m D_n+A^{(3)}_n D_n+A^{(4)}_n=0, \tag{A23}$$

$$\sum_m B^{(1)}_{mn}G_m D_m D_n+\sum_m B^{(2)}_{mn}G_m D_m+\sum_m B^{(3)}_{mn}D_m G_n +\sum_m B^{(4)}_{mn}D_m+B^{(5)}_n G_n+B^{(6)}_n=0, \tag{A24}$$

where parameters $A^{(i)}_{mn}(i=1-4)$ and $B^{(i)}_{mn}(i=1-6)$ are directly related to the parameters of the potential model (2),

$$A^{(1)}_{nm}=\frac{2\pi}{z_n^2}\rho^2 C^{(a)}_{nm}, \tag{A25}$$

$$A^{(2)}_{nm}=\rho D^{(a)}_{nm}, \tag{A26}$$

$$A^{(3)}_n=\frac{1}{z_n^3}\rho H^{(a)}_n-1, \tag{A27}$$

$$A^{(4)}_n=2\pi e_n K_n, \tag{A28}$$

$$B^{(1)}_{nm}=\frac{2\pi}{z_n}\rho^2 C^{(a)}_{nm}, \tag{A29}$$

$$B^{(2)}_{nm}=\frac{2\pi}{z_n^2}\rho C^{(b)}_{nm}, \tag{A30}$$

$$B^{(3)}_{nm}=\rho D^{(a)}_{nm}, \tag{A31}$$

$$B^{(4)}_{nm}=D^{(b)}_{nm}, \tag{A32}$$

$$B^{(5)}_n=\frac{1}{z_n^3}\rho H^{(a)}_n-1, \tag{A33}$$

$$B^{(6)}_n=\frac{1}{2\pi}H^{(b)}_n. \tag{A34}$$

Here,

$$H^{(a)}_n=z_n b^{(0)}\theta_1(z_n\sigma)+A^{(0)}\theta_2(z_n\sigma), \tag{A35}$$

$$G^{(a)}_n=z_n A^{(0)}\theta_1(z_n\sigma)-\frac{4}{\sigma^2}B^{(0)}\theta_2(z_n\sigma), \tag{A36}$$

$$F^{(a)}_{nm}=L^{(a)}_n G^{(a)}_m-z_n M^{(a)}_n H^{(a)}_m, \tag{A37}$$

$$E^{(a)}_{nm}=G^{(a)}_m-z_n H^{(a)}_m, \tag{A38}$$

$$D^{(a)}_{nm}=\frac{1}{z_n^3 z_m^3}\left[\rho F^{(a)}_{nm}+z_n^2 z_m^2\left(1-\frac{z_n e_m}{z_n+z_m}\right)\right], \tag{A39}$$

$$C^{(a)}_{nm}=\frac{1}{z_n^3 z_m^3}\left\{\rho(E^{(a)}_{nm}-F^{(a)}_{nm}e_n)+\frac{z_n^2 z_m^2}{z_n+z_m}\times[z_m(1-e_n)-z_n e_n(1-e_m)]\right\}, \tag{A40}$$

$$H^{(b)}_n=b^{(0)}+\frac{1}{z_n}A^{(0)}, \tag{A41}$$

$$G^{(b)}_n=A^{(0)}-\frac{4}{z_n\sigma^2}B^{(0)}, \tag{A42}$$

$$F^{(b)}_{nm}=L^{(a)}_n G^{(b)}_m-z_n M^{(a)}_n H^{(b)}_m, \tag{A43}$$

$$E^{(b)}_{nm}=G^{(b)}_m-z_n H^{(b)}_m, \tag{A44}$$

$$D^{(b)}_{nm}=\frac{1}{2\pi}\left[\frac{1}{z_n^3}\rho F^{(b)}_{nm}+\frac{z_m}{z_n+z_m}\right], \tag{A45}$$

$$C^{(b)}_{nm}=\frac{1}{2\pi z_n^3}\left[\rho(E^{(b)}_{nm}-F^{(b)}_{nm}e_n)-\frac{z_m z_n^3}{z_n+z_m}e_n\right]. \tag{A46}$$

In the expressions (A35) and (A36) the functions $\theta_1(x)$ and $\theta_2(x)$ are

$$\theta_1(x)=1-x-e^{-x}, \tag{A47}$$

$$\theta_2(x)=1-x+\tfrac{1}{2}x^2-e^{-x}. \tag{A48}$$

Finally for G'_n we have

$$G'_n=\frac{2\pi\rho G_n\hat{Q}'_n-R_n}{2\pi(1-\rho\hat{Q}_n)}, \tag{A49}$$

where

$$\hat{Q}_n=\sum_m (C^{(a)}_{mn}f_m+D^{(a)}_{mn}D_m)+\frac{1}{z_n^3}H^{(a)}_n, \tag{A50}$$

$$R_n=\frac{2+z_n\sigma}{z_n^2}A^{(Y)}+\frac{1+z_n\sigma}{z_n}b-\sum_m\frac{z_n+z_n(z_n+z_m)\sigma}{(z_n+z_m)^2}C_m, \tag{A51}$$

$$\hat{Q}'_n=-\frac{A^{(Y)}}{2z_n^4}[6+\psi_3(z_n,\sigma)e_n]+\frac{1}{z_n^3}(A^{(Y)}\sigma-b)\times[2+\psi_2(z_n,\sigma)e_n]-\sum_m\frac{1}{z_m(z_n+z_m)^2}f_m-\frac{1}{z_n^2}\left(\frac{1}{2}A^{(Y)}\sigma^2-b\sigma-\sum_m\frac{1}{z_m}C_m\right)\times[1+\psi_1(z_n,\sigma)e_n]-\sum_m\frac{1}{z_m(z_n+z_m)^2}\times C_m\psi_1(z_n+z_m,\sigma)e_n, \tag{A52}$$

and the functions $\psi_1(x)$, $\psi_2(x)$, and $\psi_3(x)$ are defined by the following recursive relation:

$$\psi_i(x,y)=i\,\psi_{i-1}(x,y)-(xy)^i \tag{A53}$$

with $\psi_0(x,y) = -1$.

[1] Y. V. Kalyuzhnyi, C.-T. Lin, G. Stell, and A. Yethiraj, J. Mol. Liq. **323**, 85 (2001).
[2] C. McCabe, Y. V. Kalyuzhnyi, and P. T. Cummings, Fluid Phase Equilib. **194–197**, 185 (2002).
[3] Y. V. Kalyuzhnyi, C. McCabe, and P. T. Cummings, Mol. Phys. **100**, 2499 (2002).
[4] M. F. Holovko and Y. V. Kalyuzhnyi, Mol. Phys. **73**, 1145 (1991).
[5] Y. V. Kalyuzhnyi and M. F. Holovko, Mol. Phys. **80**, 1165 (1993).
[6] Y. V. Kalyuzhnyi and G. Stell, Chem. Phys. Lett. **240**, 157 (1995).
[7] Y. V. Kalyuzhnyi, Mol. Phys. **94**, 735 (1998).
[8] Y. V. Kalyuzhnyi and P. T. Cummings, J. Chem. Phys. **103**, 3265 (1995).
[9] Y. V. Kalyuzhnyi, C.-T. Lin, and G. Stell, J. Chem. Phys. **106**, 1940 (1997).
[10] C.-T. Lin, Y. V. Kalyuzhnyi, and G. Stell, J. Chem. Phys. **108**, 6513 (1998).
[11] Y. V. Kalyuzhnyi, C.-T. Lin, and G. Stell, J. Chem. Phys. **108**, 6525 (1998).
[12] M. S. Wertheim, J. Stat. Phys. **35**, 1935 (1984).
[13] M. S. Wertheim, J. Stat. Phys. **42**, 477 (1986); **42**, 495 (1986).
[14] W. G. Chapman, K. E. Gubbins, G. Jackson, and M. Radosz, Fluid Phase Equilib. **52**, 31 (1989).
[15] W. G. Chapman, K. E. Gubbins, G. Jackson, and M. Radosz, Ind. Eng. Chem. Res. **29**, 1709 (1990).
[16] A. Gil-Villegas, A. Galindo, P. J. Whitehead, S. J. Mills, and G. Jackson, J. Chem. Phys. **106**, 4168 (1997).
[17] L. A. Davies, A. Gil-Villegas, and G. Jackson, J. Chem. Phys. **111**, 8659 (1999).
[18] J. Chang and S. I. Sandler, Chem. Eng. Sci. **49**, 2777 (1994).
[19] D. Ghonasgi and W. G. Chapman, J. Chem. Phys. **100**, 6633 (1994).
[20] M. S. Wertheim, J. Chem. Phys. **87**, 7323 (1987).
[21] M.-J. Lee, C. McCabe, and P. T. Cummings, Fluid Phase Equilib. **221**, 63 (2004).
[22] C. McCabe, A. Galindo, A. Gil-Villegas, and G. Jackson, Int. J. Thermophys. **19**, 1511 (1998).
[23] C. McCabe, A. Galindo, A. Gil-Villegas, and G. Jackson, J. Phys. Chem. B **102**, 8060 (1998).
[24] A. Galindo, A. Gil-Villegas, P. J. Whitehead, G. Jackson, and A. N. Burgess, J. Phys. Chem. B **102**, 7632 (1998).
[25] C. McCabe, A. Gil-Villegas, and G. Jackson, J. Phys. Chem. B **102**, 4183 (1998).
[26] A. Galindo, L. J. Florusse, and C. J. Peters, Fluid Phase Equilib. **160**, 123 (1999).
[27] C. McCabe and G. Jackson, Phys. Chem. Chem. Phys. **1**, 2057 (1999).
[28] Z. Y. Sun, L. J. An, H. F. Li, Z. H. Jiang, and Z. W. Wu, Macromol. Theory Simul. **10**, 692 (2001).
[29] C. McCabe, A. Galindo, M. N. Garcia-Lisbona, and G. Jackson, Ind. Eng. Chem. Res. **40**, 3835 (2001).
[30] P. Paricaud, A. Galindo, and G. Jackson, Fluid Phase Equilib. **194–197**, 87 (2002).
[31] F. J. Blas and A. Galindo, Fluid Phase Equilib. **194–197**, 501 (2002).
[32] A. Galindo and F. J. Blas, J. Phys. Chem. B **106**, 4503 (2002).
[33] J. A. Barker and D. Henderson, J. Chem. Phys. **47**, 2856 (1967).
[34] J. A. Barker and D. Henderson, J. Chem. Phys. **47**, 4714 (1967).
[35] A. Malijevsky and S. Labk, Mol. Phys. **60**, 663 (1987).
[36] D. Henderson, L. Blum, and J. P. Noworyta, J. Chem. Phys. **102**, 4973 (1995).
[37] L. Blum and J. S. Høye, J. Stat. Phys. **19**, 317 (1978).
[38] J. S. Høye and G. Stell, J. Chem. Phys. **67**, 439 (1977).
[39] E. Arrieta, C. Jedrzejek, and K. N. Marsh, J. Chem. Phys. **95**, 6806 (1991).
[40] F. A. Escobedo and J. J. de Pablo, J. Chem. Phys. **103**, 1946 (1995).
[41] G. Stell, C.-T. Lin, and Y. V. Kalyuzhnyi, J. Chem. Phys. **110**, 5444 (1999); **110**, 5458 (1999).
[42] D. Frenkel and B. Smit, *Understanding Molecular Simulation: from Algorithms to Applications* (Academic Press, San Diego, 2001).
[43] X.-Y. Wang and Y. C. Chiew, J. Chem. Phys. **115**, 4376 (2001).
[44] E. Lomba, Mol. Phys. **68**, 87 (1989).
[45] L. Belloni, J. Chem. Phys. **98**, 8080 (1993).
[46] J. S. Høye, E. Lomba, and G. Stell, Mol. Phys. **79**, 523 (1993).